

Behavior of Impurity Ion Velocities during the Pulsed Poloidal Current Drive in the Madison Symmetric Torus Reversed-Field Pinch

Hajime SAKAKITA*, Darren CRAIG¹, Jay K. ANDERSON¹, Ted M. BIEWER²,
Stephen D. TERRY², Brett E. CHAPMAN¹, Daniel J. DEN-HARTOG¹ and Stewart C. PRAGER¹

Energy Electronics Institute, National Institute of Advanced Industrial Science and Technology (AIST), 1-1-1 Umezono, Tsukuba 305-8568, Japan

¹*Department of Physics, University of Wisconsin-Madison, 1150 University Avenue, Madison 53706, U.S.A.*

²*Princeton Plasma Physics Laboratory, Princeton University, P.O.Box 451, Princeton 08543-0451, U.S.A.*

(Received March 25, 2003; accepted for publication April 9, 2003)

We report on passive measurements of impurity ion velocities during the pulsed poloidal current drive (PPCD) in the Madison Symmetric Torus reversed-field pinch. During PPCD, the electron temperature increased and a sudden reduction of magnetic fluctuations was observed. For this change, we have studied whether plasma velocity is affected. Plasma rotation is observed to decrease during PPCD. From measurements of line intensities for several impurities at 10 poloidal chords, it is found that the impurity line emission shifts outward. The ion temperature of impurities is reasonably connected to that measured by charge exchange recombination spectroscopy from core to edge. [DOI: 10.1143/JJAP.42.L505]

KEYWORDS: plasma velocity, ion temperature, impurity emission, equilibrium reconstruction, pulsed poloidal current drive, reversed field pinch

The reversed-field pinch (RFP) has attractive features as a fusion reactor, since the plasma is confined by weak toroidal magnetic fields. However, RFP plasmas are susceptible to large-amplitude magnetic field fluctuations. These fluctuations grow to an amplitude sufficient to cause reconnection and stochasticization of the magnetic field lines, thereby degrading the energy confinement. In order to decrease these fluctuations, a pulsed poloidal current drive (PPCD) was applied to replace the dynamo electric field in the Madison Symmetric Torus (MST) RFP (major and minor radii, $R/a = 1.5\text{ m}/0.52\text{ m}$).¹⁾ As a result, the magnetic fluctuations with poloidal mode numbers $m = 1$ and $m = 0$ have been further suppressed, and a considerable increase of energy confinement has been achieved.²⁾ In the initial stage of PPCD, accompanying the sudden reduction of both magnetic fluctuations and radiation from neutral deuterium atoms, the electron temperature increased rapidly.²⁾ This improvement may be connected with a current profile change to a more stable region.^{3,4)} In tokamaks, H-mode transitions have been induced by changes in the flow profile.⁵⁾ Therefore, we are attempting to measure spectroscopically the toroidal velocity component of the radial electric field in order to confirm or deny the probe measurements that were previously published.⁶⁾ We have also gained insight into whether or not a transport barrier due to a local velocity shear causes the electron temperature to increase.

In order to obtain a toroidal plasma velocity profile, we have measured the Doppler shift of several impurity lines using the ion dynamics spectrometer (IDS) precisely described in ref. 7. (Charge exchange recombination spectroscopy (CHERS) is not applicable for toroidal plasma velocity measurement at present.) This spectrometer is applicable to measure impurity ion temperature and flow velocities simultaneously with $10\ \mu\text{s}$ temporal resolution. This device is actually a duo-spectrometer: measurements from two toroidally different chordal views of the plasma can be made simultaneously via two separate quartz input fiber optic bundles coupled to the entrance slit of the spectrometer. We measured flow velocities and ion tem-

perature for CV (227.1 nm), BIV (282.3 nm), OV (278.1 nm), CIII (229.6 nm) and HeII (468.6 nm) lines. Measurements of toroidal flow are line-averaged along the viewing chord which samples the plasma from $r/a = 0.3$ to 1.0. A measurement of impurity ion temperature is also observed from these data.

To measure the radial emission location, line intensities for each impurity species were measured at 10 poloidal viewing chords of the impact parameter $r/a = -0.87, -0.58, -0.41, -0.24, -0.09, 0.10, 0.28, 0.45, 0.62$ and 0.839 , as shown in Fig. 1. The $r/a = -0.87$ and 0.839 chords are toroidally 120 deg. apart from the other 8 chords. The data are inverted by means of the equilibrium reconstruction code (MSTFit) in order to obtain the radial emission profiles.⁸⁾

The plasma current, I_p was $\sim 210\text{ kA}$, and the PPCD trigger timing was fixed at $t = 9.0\text{ ms}$. The soft X-ray (SXR) ratio (beryllium filter, $15\ \mu\text{m}/7.5\ \mu\text{m}$) that corresponds to electron temperature (T_e) increases after a sawtooth crash at $t \sim 11\text{ ms}$ as shown in Fig. 2. Figures 3(a)–3(c) show the

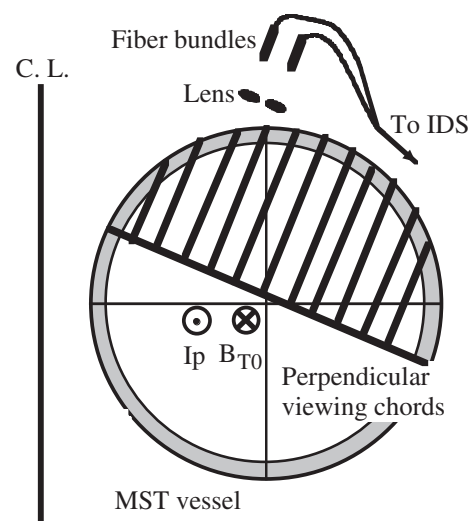


Fig. 1. Cross-sectional view of MST and perpendicular viewing chords. Directions of plasma current and core toroidal magnetic field are indicated.

*E-mail address: h.sakakita@aist.go.jp

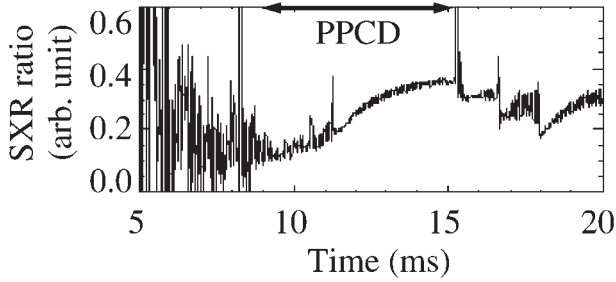


Fig. 2. Time behavior of the ratio of two SXR measurements, which is the indication of $T_e(t)$.

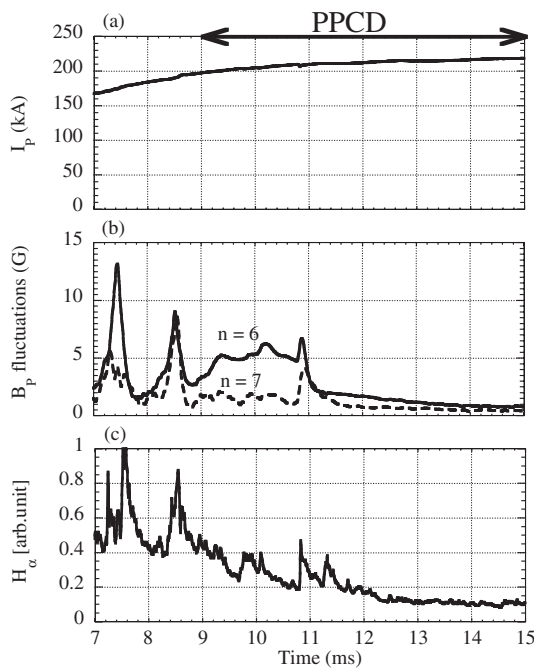


Fig. 3. (a) Plasma current, (b) magnetic mode amplitudes of $n = 6$ and 7 and (c) H_α emission.

time behaviors of I_p , magnetic mode amplitudes and H_α , respectively. After the start of PPCD, a state dominated by toroidal mode number $m = 1/n = 6$ is formed. After the final SXR crash ($t \sim 11$ ms), both magnetic fluctuations and radiation from neutral deuterium atoms decrease. Hereafter, we consider the moments immediately before and after the SXR crash, i.e., $t = 10.5$ and 13.5 ms.

Electron density profiles measured by a far infrared interferometer are shown in Fig. 4.⁴⁾ At $t = 13.5$ ms, the electron density gradient becomes steeper at $r/a \sim 0.7$. The electron temperature gradient also became steep at $r/a \sim 0.7$ as shown in Fig. 7 of ref. 2.

Figure 5 shows the measured toroidal plasma velocities (V_{toroidal}) and ion temperatures (T_i) for CV, BIV, OV, HeII and CIII. A 100 μs moving average and also a shot average were conducted. Toroidal plasma rotation gradually decreased during PPCD. Here, the positive sign indicates plasma current direction. Ion temperatures of CV, HeII and CIII show almost no change, while ion temperatures of BIV and OV decrease with PPCD.

Figures 6(a)–6(c) show the line integrated emission profiles (open symbols). Solid symbols represent the

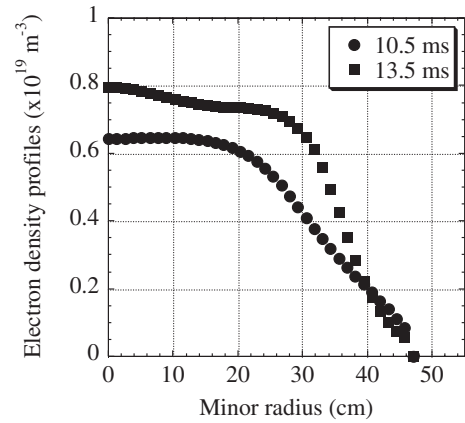


Fig. 4. Electron density profiles at $t = 10.5$ ms (solid circle) and 13.5 ms (solid square).

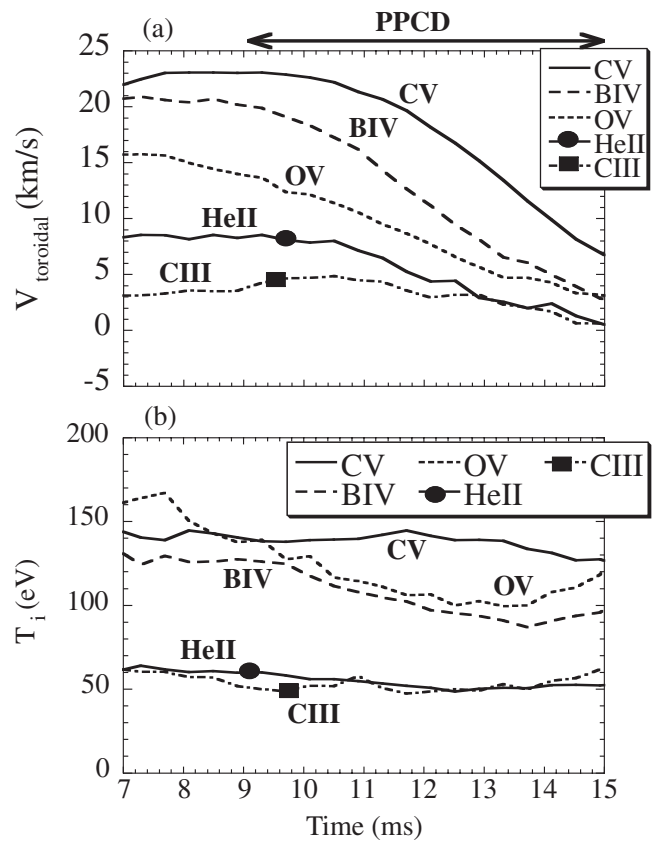


Fig. 5. Smoothed time behavior of (a) toroidal plasma velocities and (b) ion temperatures. Solid line (CV), broken line (BIV), dashed line (OV), solid line with solid circle (HeII) and dashed line with solid square (CIII).

calculated line integral data from Abel inverted emission profiles (solid lines) shown in Figs. 6(d)–6(f). Inverted data fits the raw data fairly well as shown in Figs. 6(a)–6(c). Line integrated and inverted emission profiles indicate the outward shift of the peak emission with increased electron temperature from PPCD as shown in Fig. 6. I^*W curves (broken lines in Figs. 6(d)–6(f)) indicate radial emission profiles multiplied by the appropriate toroidal geometric sensitivity function, W , as defined in ref. 9. To identify a typical location of each species, equation, $\langle r \rangle = \int Iwrdr / \int IWdr$, is adopted in the integration range of 0.4 to 1.0.

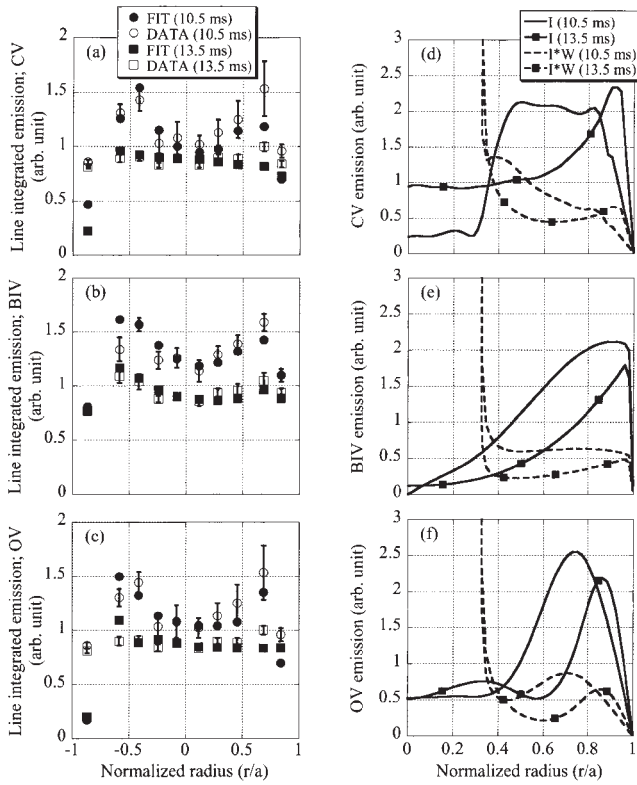


Fig. 6. Line integrated emission profiles at $t = 10.5$ and 13.5 ms, (a) CV, (b) BIV and (c) OV. Inverted radial emission profiles and radial emission profiles multiplied by the appropriate geometric sensitivity function, (d) CV, (e) BIV and (f) OV.

Since a helium gas puffing port was close to the poloidal viewing chord used, the HeII emission could not be inverted reliably.

Figure 7(a) shows toroidal plasma velocity profiles. Measured species are shifted to $r/a > 0.7$ during PPCD. The shear in the plasma rotation is unclear due to the insufficient spatial resolution, particularly inside $r/a \sim 0.7$. However, we can see a slight velocity gradient around $r/a \sim 0.7$ at $t \sim 13.5$ ms. Figure 7(b) shows ion temperature profiles from the passive measurement as well as the C^{5+} ion temperature profile using CHERS.^{2,10} Although the uncertainty in the ion location is large, a slight pedestal of ion temperature around $r/a \sim 0.7$ is indicated at $t \sim 13.5$ ms.

In summary, we have measured the Doppler shift of several impurity lines in order to obtain a toroidal velocity profile in the initial stage of PPCD. Radial emission profiles for each impurity species have been measured using 10 poloidal chords. Due to the insufficient spatial resolution, any changes in the plasma rotation profile are unclear. However, the ion temperature profile is obtained from core to edge during PPCD. Improvement of the spatial resolution using CHERS for velocity profile and ion temperature, and study of the correlation of the velocity shear with local fluctuations are future problems.¹¹

This work was supported by USDOE.

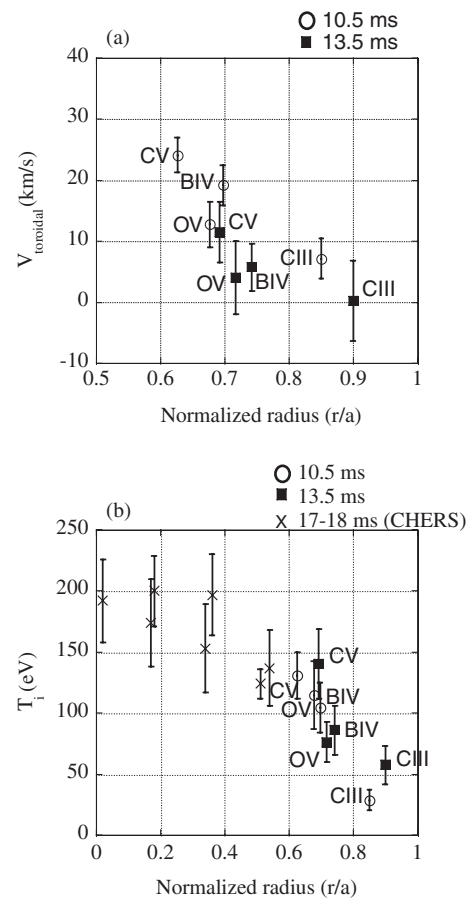


Fig. 7. (a) Toroidal plasma rotation profiles and (b) ion temperature profiles at $t = 10.5$ and 13.5 ms. CIII location is assumed to be $r/a = 0.85$ ($t = 10.5$ ms) and 0.9 ($t = 13.5$ ms), respectively. For reference, the ion temperature profile measured by CHERS is also shown.

- 1) J. S. Sarff, S. A. Hokin, H. Ji, S. C. Prager and C. R. Sovinec: Phys. Rev. Lett. **72** (1994) 3670.
- 2) B. E. Chapman, A. F. Almagri, J. K. Anderson, T. M. Biewer, P. K. Chattopadhyay, C.-S. Chiang, D. Craig, D. J. Den Hartog, G. Fiksel, C. B. Forest, A. K. Hansen, D. Holly, N. E. Lanier, R. O'Connell, S. C. Prager, J. C. Reardon, J. S. Sarff, M. D. Wyman, D. L. Brower, W. X. Ding, Y. Jiang, S. D. Terry, P. Franz, L. Marrelli and P. Martin: Phys. Plasmas **9** (2002) 2061.
- 3) C. R. Sovinec and S. C. Prager: Nucl. Fusion **39** (1999) 777.
- 4) D. L. Brower, W. X. Ding, S. D. Terry, J. K. Anderson, T. M. Biewer, B. E. Chapman, D. Craig, C. B. Forest, S. C. Prager and J. S. Sarff: Phys. Rev. Lett. **88** (2002) 185005.
- 5) H. Kimura and the JT-60 Team: Phys. Plasmas **3** (1996) 1943.
- 6) B. E. Chapman, A. F. Almagri, J. K. Anderson, C.-S. Chiang, D. Craig, G. Fiksel, N. E. Lanier, S. C. Prager, J. S. Sarff, M. R. Stoneking and P. W. Terry: Phys. Plasmas **5** (1998) 1848.
- 7) D. J. Den Hartog and R. J. Fonck: Rev. Sci. Instrum. **65** (1994) 3238.
- 8) J. K. Anderson: Dr. Thesis, Department of Physics, University of Wisconsin, Madison, 2001.
- 9) D. J. Den Hartog, J. T. Chapman, D. Craig, G. Fiksel, P. W. Fontana, S. C. Prager and J. S. Sarff: Phys. Plasmas **6** (1999) 1813.
- 10) D. Craig, D. J. Den Hartog, G. Fiksel, V. I. Davydenko and A. A. Ivanov: Rev. Sci. Instrum. **72** (2001) 1008.
- 11) N. E. Lanier, D. Craig, J. K. Anderson, T. M. Biewer, B. E. Chapman, D. J. Den Hartog, C. B. Forest, S. C. Prager, D. L. Brower and Y. Jiang: Phys. Plasmas **8** (2001) 3402.